



## Original article

## Binding sites of retinol and retinoic acid with serum albumins

A. Belatik<sup>a</sup>, S. Hotchandani<sup>a</sup>, J. Bariyanga<sup>b</sup>, H.A. Tajmir-Riahi<sup>a,\*</sup><sup>a</sup> Département de Chimie-Biologie, Université du Québec à Trois-Rivières, C. P. 500, Trois-Rivières (Québec), G9A 5H7, Canada<sup>b</sup> Department of Chemistry, University of Hawaii-West O'ahu, 96-129 Ala Ike, Pearl City, HI 96782, USA

## ARTICLE INFO

## Article history:

Received 26 July 2011

Received in revised form

27 November 2011

Accepted 2 December 2011

Available online 9 December 2011

## Keywords:

Retinoid

BSA

HSA

Spectroscopy

Modeling

## ABSTRACT

Retinoids are effectively transported in the bloodstream *via* serum albumins. We report the complexation of bovine serum albumin (BSA) with retinol and retinoic acid at physiological conditions, using constant protein concentration and various retinoid contents. FTIR, CD and fluorescence spectroscopic methods and molecular modeling were used to analyze retinoid binding site, the binding constant and the effects of complexation on BSA stability and secondary structure. Structural analysis showed that retinoids bind BSA *via* hydrophilic and hydrophobic interactions with overall binding constants of  $K_{\text{Ret-BSA}} = 5.3 (\pm 0.8) \times 10^6 \text{ M}^{-1}$  and  $K_{\text{Retac-BSA}} = 2.3 (\pm 0.4) \times 10^6 \text{ M}^{-1}$ . The number of bound retinoid molecules ( $n$ ) was  $1.20 (\pm 0.2)$  for retinol and  $1.8 (\pm 0.3)$  for retinoic acid. Molecular modeling showed the participation of several amino acids in retinoid–BSA complexes stabilized by H-bonding network. The retinoid binding altered BSA conformation with a major reduction of  $\alpha$ -helix from 61% (free BSA) to 36% (retinol–BSA) and 26% (retinoic acid–BSA) with an increase in turn and random coil structures indicating a partial protein unfolding. The results indicate that serum albumins are capable of transporting retinoids *in vitro* and *in vivo*.

© 2011 Elsevier Masson SAS. All rights reserved.

## 1. Introduction

13-*cis* Retinoic acid (Scheme 1) is rapidly absorbed into cells and exerts its anti-proliferative effect on human sebocytes by specific isomerization to high levels of all-*trans* retinoic acid, while binding the retinoic acid receptors [1]. Several retinol binding proteins are identified and structurally characterized [2–5]. It has been suggested that the addition of high concentration of bovine serum albumin controls the uptake of 13-*cis* and all *trans*-retinoic acid in cell and reduces significantly the isomerization of all *cis*-retinoic acid to all *trans*-retinoic acid [1]. However, the mechanism by which serum albumins alter the activity of retinol and retinoic acid is not well understood.

Serum albumins are constituents of the circulatory system and have many physiological functions [6]. The most important property of this group of proteins is that they serve as transporters for a variety of compounds including retinoids. BSA (Scheme 1) has been one of the most extensively studied of this group of proteins, particularly because of its structural homology with human serum albumin (HSA). The BSA molecule is made up of three homologous

domains (I, II, III) that are divided into nine loops (L1–L9) by 17 disulfide bonds. The loops in each domain are made up of a sequence of large–small–large loops forming a triplet. Each domain in turn is the product of two subdomains (IA, IB, etc.). X-ray-crystallographic data [7,8] show that the albumin structure is predominantly  $\alpha$ -helical with the remaining polypeptide, occurring in turns and in extended or flexible regions between subdomains with no  $\beta$ -sheets. BSA has two tryptophan residues that possess intrinsic fluorescence [9,10]. Trp-134 in the first domain and Trp-212 in the second domain. Trp-212 is located within a hydrophobic binding pocket of the protein and Trp-134 is located on the surface of the molecule. While there are marked similarities between BSA and HSA in their compositions, HSA has only one tryptophan residue Trp-214, while BSA contains two tryptophans Trp-212 and Trp-134 as fluorophores capable of fluorescence quenching.

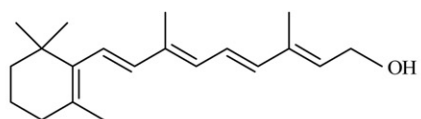
Fluorescence quenching is considered as a technique for measuring binding affinities. Fluorescence quenching is the decrease of the quantum yield of fluorescence from a fluorophores induced by a variety of molecular interactions with quencher molecule [11]. Therefore, it was of interest to use quenching of the intrinsic tryptophan fluorescence of BSA as a tool to study the interaction of retinol and retinoic acid with BSA in an attempt to characterize the nature of retinoid–protein complexation.

We report the spectroscopic analysis of BSA complexes with retinol and retinoic acid in aqueous solution at physiological conditions, using constant protein concentration and various

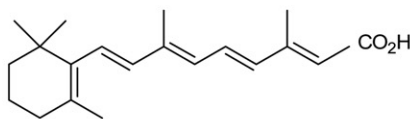
Abbreviations: BSA, bovine serum albumin; HSA, human serum albumin; ret, retinol; retac, retinoic acid; FTIR, Fourier transform infrared spectroscopy; CD, circular dichroism.

\* Corresponding author. Tel.: +1 819 376 5011x3310; fax: +1 819 376 5084.

E-mail address: [tajmirri@uqtr.ca](mailto:tajmirri@uqtr.ca) (H.A. Tajmir-Riahi).

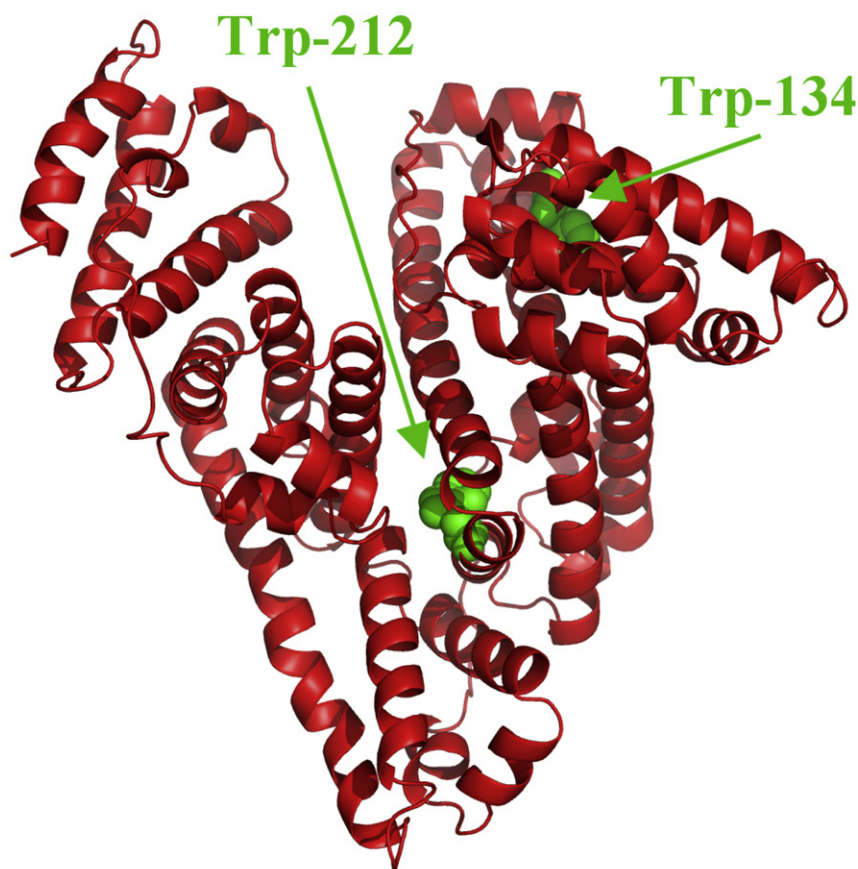


All-trans retinol



All-trans retinoic acid

Chemical structures of retinol and retinoic acid



3D structure of bovine serum albumin showing Trp-212 and Trp-134 in green color

Scheme 1.

retinoid contents. Structural information regarding retinoid binding sites and the effect of retinoid–BSA complexation on the protein stability and secondary structure is reported. Furthermore, a comparison between retinol and retinoic acid complexes with BSA and HSA was made here.

## 2. Experimental section

### 2.1. Materials

BSA fraction V and all *trans*-retinol and all *trans*-retinoic acid were purchased from Sigma Chemical Company and used as

supplied. Other chemicals were of reagent grade and used without further purification.

### 2.2. Preparation of stock solutions

Bovine serum albumin was dissolved in aqueous solution (40 mg/ml or 0.5 mM) containing 10 mM Tris–HCl buffer (pH 7.4). The protein concentration was determined spectrophotometrically using the extinction coefficient of  $36\,500\text{ M}^{-1}\text{ cm}^{-1}$  at 280 nm [12]. Retinoid solution (1 mM) was first prepared in Tris–HCl/ethanol 50% and then diluted by serial dilution in Tris–HCl/ethanol 50%. After addition of equal volume of retinoid solution to protein

solution, the final ethanol concentration was reduced to 25%. The presence of 25% of ethanol induces no major BSA structural changes according to literature report [13]. More detailed study regarding the effect of 25% ethanol on BSA conformation will be discussed in the text further on.

### 2.3. FTIR spectroscopic measurements

Infrared spectra were recorded on a FTIR spectrometer (Impact 420 model), equipped with deuterated triglycine sulfate (DTGS) detector and KBr beam splitter, using AgBr windows. Solution of retinoid was added dropwise to the BSA solution with constant stirring to ensure the formation of homogeneous solution and to have retinoid concentrations of 0.125, 0.25 and 0.5 mM with a final protein concentration of 0.25 mM (20 mg/ml in 25% ethanolic solution). Spectra were collected after 2 h incubation of BSA with retinoid solution at room temperature, using hydrated films. Interferograms were accumulated over the spectral range 4000–600  $\text{cm}^{-1}$  with a nominal resolution of 2  $\text{cm}^{-1}$  and 100 scans. The difference spectra [(protein solution + retinoid solution) – (protein solution)] were generated using water combination mode around 2300  $\text{cm}^{-1}$ , as standard [14]. When producing difference spectra this band was adjusted to the baseline level, in order to normalize difference spectra.

### 2.4. Analysis of protein conformation

Analysis of the secondary structure of BSA and its retinoid complexes was carried out on the basis of the procedure previously reported [15]. The protein secondary structure is determined from the shape of the amide I band, located around 1660–1650  $\text{cm}^{-1}$ . The FT–IR spectra were smoothed and their baselines were corrected automatically using Grams AI software. Thus, the root-mean square (rms) noise of every spectrum was calculated. By means of the second derivative in the spectral region 1700–1600  $\text{cm}^{-1}$ , the major peaks for BSA and the complexes were resolved. The above spectral region was deconvoluted by the curve-fitting method with the Levenberg–Marquadt algorithm and the peaks corresponds to  $\alpha$ -helix (1658–1656  $\text{cm}^{-1}$ ),  $\beta$ -sheet (1640–1610  $\text{cm}^{-1}$ ), turn (1670–1665  $\text{cm}^{-1}$ ), random coil (1648–1641  $\text{cm}^{-1}$ ) and  $\beta$ -anti-parallel (1692–1680  $\text{cm}^{-1}$ ) were adjusted and the area was measured with the Gaussian function. The area of all the component bands assigned to a given conformation were then summed up and divided by the total area [16,17]. The curve-fitting analysis was performed using the GRAMS/AI Version 7.01 software of the Galactic Industries Corporation.

### 2.5. Circular dichroism

CD Spectra of BSA and its retinoid complexes were recorded with a Jasco J-720 spectropolarimeter. For measurements in the far-UV region (178–260 nm), a quartz cell with a path length of 0.1 cm was used in nitrogen atmosphere. BSA concentration was kept constant (12.5  $\mu\text{M}$ ), while varying each retinoid concentration (0.125, 0.25 and 0.5 mM in 25% ethanolic solution). An accumulation of three scans with a scan speed of 50 nm per minute was performed and data were collected for each nm from 260 to 180 nm. Sample temperature was maintained at 25  $^{\circ}\text{C}$  using a Neslab RTE-111 circulating water bath connected to the water-jacketed quartz cuvettes. Spectra were corrected for buffer signal and conversion to the Mol CD ( $\Delta\epsilon$ ) was performed with the Jasco Standard Analysis software. The protein secondary structure was calculated using CDSSTR, which calculates the different assignments of secondary structures by comparison with CD spectra, measured from different proteins for which high quality X-ray

diffraction data are available [18,19]. The program CDSSTR is provided in CDPro software package which is available at the website: <http://lamar.colostate.edu/~sreeram/CDPro>.

### 2.6. Fluorescence spectroscopy

Fluorometric experiments were carried out on a Varian Cary Eclipse. Stock solutions of retinoid 1 mM in buffer (pH = 7.4) were prepared at room temperature ( $24 \pm 1$   $^{\circ}\text{C}$ ). Various solutions of retinoid (2–60  $\mu\text{M}$ ) were prepared in 10% ethanolic solution from the above stock solutions by successive dilutions also at  $24 \pm 1$   $^{\circ}\text{C}$ . Solution of BSA (15  $\mu\text{M}$ ) in 10 mM Tris–HCl (pH. 7.4) was also prepared at  $24 \pm 1$   $^{\circ}\text{C}$ . The above solutions were kept in the dark and used soon after. Samples containing 2 ml of the above BSA solution and 2 ml of various retinoid solutions were mixed to obtain final retinoid concentrations of 1–60  $\mu\text{M}$  with constant BSA content 7.5  $\mu\text{M}$ . The fluorescence spectra were recorded at  $\lambda_{\text{exc}} = 280$  nm and  $\lambda_{\text{em}}$  from 287 to 500 nm. The intensity at 340 nm (tryptophan) was used to calculate the binding constant ( $K$ ) according to literature reports [20–25].

On the assumption that there are ( $n$ ) substantive binding sites for quencher ( $Q$ ) on protein ( $B$ ), the quenching reaction can be shown as follows:



The binding constant ( $K_A$ ), can be calculated as:

$$K_A = [Q_nB]/[Q]^n[B] \quad (2)$$

where,  $[Q]$  and  $[B]$  are the quencher and protein concentration, respectively,  $[Q_nB]$  is the concentration of non fluorescent fluorophore–quencher complex and  $[B_0]$  gives total protein concentration:

$$[Q_nB] = [B_0] - [B] \quad (3)$$

$$K_A = ([B_0] - [B])/[Q]^n[B] \quad (4)$$

The fluorescence intensity is proportional to the protein concentration as described:

$$[B]/[B_0] \propto F/F_0 \quad (5)$$

Results from fluorescence measurements can be used to estimate the binding constant of retinoid–protein complex. From Eq. (4):

$$\log[(F_0 - F)/F] = \log K_A + n \log [Q] \quad (6)$$

The accessible fluorophore fraction ( $f$ ) can be calculated by modified Stern–Volmer equation:

$$F_0/(F_0 - F) = 1/fK[Q] + 1/f \quad (7)$$

where,  $F_0$  is the initial fluorescence intensity and  $F$  is the fluorescence intensities in the presence of quenching agent (or interacting molecule).  $K$  is the Stern–Volmer quenching constant,  $[Q]$  is the molar concentration of quencher and  $f$  is the fraction of accessible fluorophore to a polar quencher, which indicates the fractional fluorescence contribution of the total emission for an interaction with a hydrophobic quencher [11].

### 2.7. Molecular modeling and docking

Structure of BSA was predicted by automated homology modeling using SWISS-MODEL Workspace from the amino acid sequence NP-851335 [26,27]. The structure of free HSA (PDB id:

1AO6, chain A) obtained by X-ray crystallography was used as a template [28]. These two proteins share 78.1% of sequence identity, which is sufficient to obtain reliable sequence alignment [29]. Images of the structures were generated using Pymol (DeLano Scientific, Palo Alto, CA, USA). RMSD between model and template proteins was 0.20 Å for positions of backbone atoms, as calculated with DeepView/Swiss-PdbViewer 4.0.1 (Scheme 1). The quality of the predicted BSA structure was found to be similar to the structure of free HSA used here as a template, using structure and model assessment tools of SWISS-MODEL workspace.

The docking studies were performed with ArgusLab 4.0.1 software (Mark A. Thompson, Planaria Software LLC, Seattle, Wa, <http://www.arguslab.com>). The structure of BSA was obtained from the above method and three dimensional structure of retinoid was generated from PM3 semi-empirical calculations, using Chem3D Ultra 6.0. A blind docking approach was taken as the whole protein was selected as a potential binding site. The docking runs were performed on the ArgusDock docking engine using high precision with a maximum of 200 candidate poses. The conformations were ranked using the Ascore scoring function, which estimates the free binding energy. Upon location of the potential binding sites, the docked complex conformations were optimized using a steepest descent algorithm until convergence, within 40 iterations. Amino

acid residues within a distance of 3.5 Å relative to retinol or retinoic acid were involved in the complexation. Water was removed from the protein binding site in order to dock the ligand at that site.

### 3. Results and discussion

#### 3.1. FTIR spectra of retinoid–BSA complexes

The retinoid–BSA interaction was characterized by infrared spectroscopy and its derivative methods. Since there was no major spectral shifting for the protein amide I band at  $1656\text{ cm}^{-1}$  (mainly C=O stretch) and amide II band at  $1545\text{ cm}^{-1}$  (C–N stretching coupled with N–H bending modes) [30,31] upon retinoid complexation, the difference spectra [(protein solution + retinoid solution) – (protein solution)] were obtained, in order to monitor the intensity variations of these vibrations and the results are shown in Fig. 1. Similarly, the infrared self-deconvolution with second derivative resolution enhancement and curve-fitting procedures [15] were used to determine the protein secondary structures in the presence of retinoids (Fig. 2 and Table 1).

At low retinoid concentration (0.125 mM), an increase in intensity was observed for the protein amide I at  $1657\text{ cm}^{-1}$  and amide II at  $1541\text{ cm}^{-1}$ , in the difference spectra of the retinol–BSA and

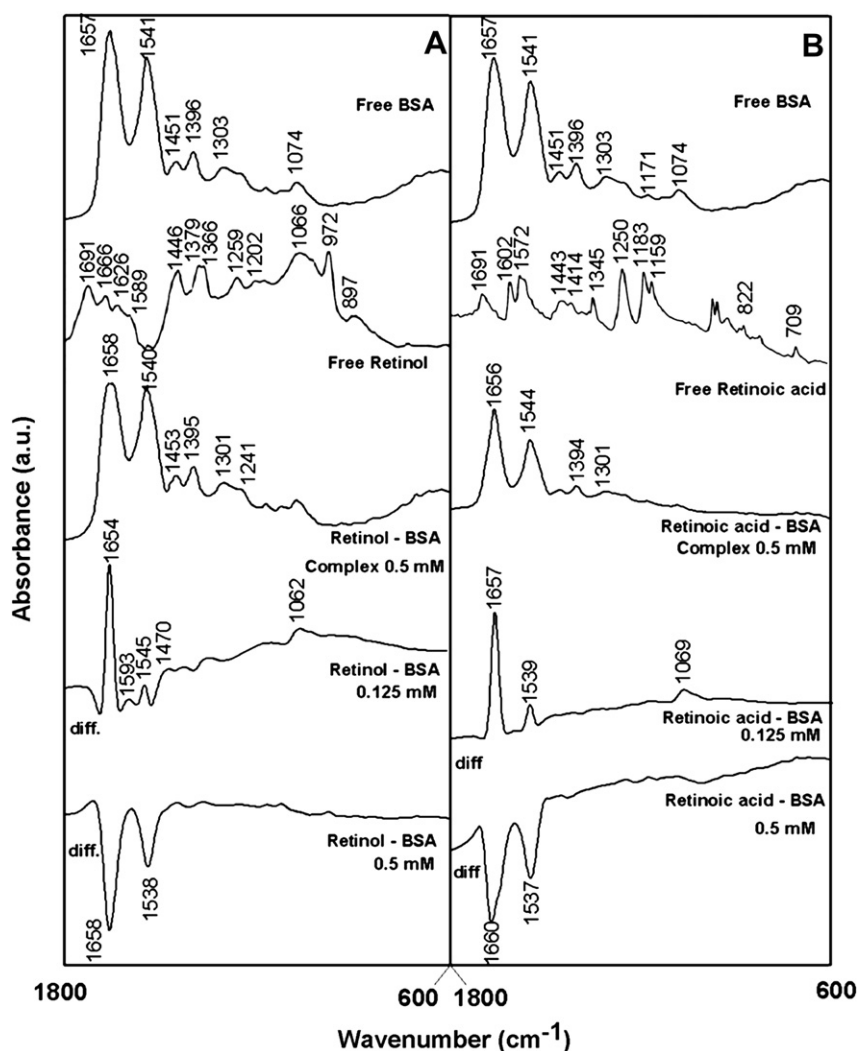


**Fig. 1.** FTIR spectra in the region of  $1800\text{--}600\text{ cm}^{-1}$  of hydrated films (pH 7.4) for free BSA (0.25 mM) and its retinoid complexes for (A) retinol and (B) retinoic acid, with difference spectra (diff.) (bottom two curves) obtained at different retinoid concentrations (indicated on the figure).



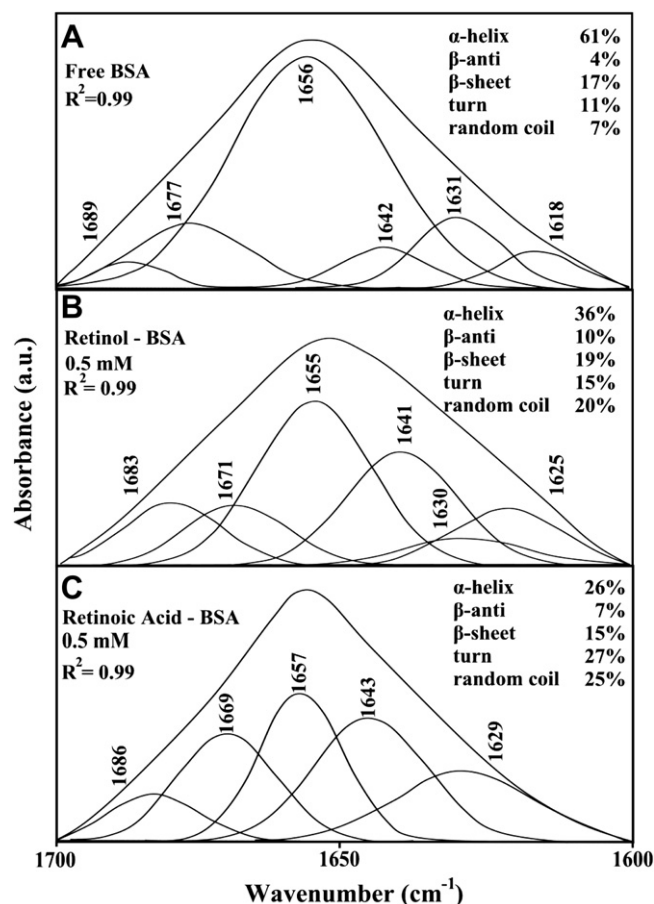


**Fig. 2.** Second derivative resolution enhancement and curve-fitted amide I region (1700–1600 cm<sup>-1</sup>) for free BSA and its retinoid complexes with 0.5 mM retinol and 0.5 mM retinoic acid.

retinoic acid–BSA complexes (Fig. 1A and B, diff. 0.125 mM). Positive features are observed in the difference spectra for amide I and II bands at 1654, 1545 cm<sup>-1</sup> (retinol), 1657 and 1539 cm<sup>-1</sup> (retinoic acid) (Fig. 1A and B, diff., 0.125 mM). These positive features are related to increase in intensity of the amide I and amide II bands upon retinoid complexation. The increase in intensity of the amide I and amide II bands is due to retinoid binding to protein C=O, C–N and N–H groups (hydrophilic interaction). Additional evidence to support the protein interaction with C–N and N–H groups comes from the shifting of the protein amide A band at 3290 cm<sup>-1</sup> (N–H stretching mode) in the free BSA to 3285 (retinol) and 3284 cm<sup>-1</sup> (retinoic acid), upon protein complexation (spectra not shown).

As retinoid concentration increased to 0.5 mM, decrease in intensity of the amide I and amide II bands were observed with negative features at 1658, 1538 cm<sup>-1</sup> (retinol), 1660 and 1537 cm<sup>-1</sup> (retinoic acid), in the difference spectra of retinoid–BSA complexes

**Table 1**  
Secondary structure analysis (infrared spectra) from the free BSA and its retinoid complexes in hydrated film at pH 7.4.

Amide I components (cm <sup>-1</sup> )	Free BSA (%) 0.5 mM	Retinol–BSA (%) 0.5 mM	Retinoic acid–BSA (%) 0.1 mM
1692–1680 $\beta$ -anti ( $\pm 1$ )	4	10	7
1680–1660 turn ( $\pm 2$ )	11	15	27
1660–1650 $\alpha$ -helix ( $\pm 3$ )	61	36	26
1648–1641 random coil ( $\pm 1$ )	7	20	25
1640–1610 $\beta$ -sheet ( $\pm 2$ )	17	19	15

**Table 2**

Secondary structure of BSA complexes (CD spectra) with retinoids at pH 7.4 calculated by CDSSTR software.

Amide I components (cm <sup>-1</sup> )	Free BSA (12.5 $\mu$ M)	Retinol–BSA (0.5 mM)	Retinoic acid–BSA (0.5 mM)
$\alpha$ -Helix (%) ( $\pm 3$ )	62	52	44
$\beta$ -Sheet (%) ( $\pm 2$ )	13	16	18
Turn (%) ( $\pm 2$ )	12	14	18
Random (%) ( $\pm 2$ )	13	18	20

(Fig. 1A and B, diff. 0.5 mM). The observed decrease in intensity of the amide I band, in the spectra of the retinoid–protein complexes suggests a major reduction of protein  $\alpha$ -helical structure at high retinoid concentrations. Similar infrared spectral changes were observed for protein amide I band in several ligand–protein complexes, where major protein conformational changes occurred [31].

A quantitative analysis of the protein secondary structure for the free BSA and its retinoid adducts in hydrated films has been carried out and the results are shown in Fig. 2 and Table 1. The free protein has 61%  $\alpha$ -helix (1656 cm<sup>-1</sup>),  $\beta$ -sheet 17% (1631 and 1618 cm<sup>-1</sup>), turn structure 11% (1677 cm<sup>-1</sup>),  $\beta$ -antiparallel 4% (1689 cm<sup>-1</sup>) and random coil 7% (1642 cm<sup>-1</sup>) (Fig. 2A and Table 1). The results are consistent with the spectroscopic studies of BSA conformation previously reported [32,33]. Upon retinoid interaction, a major decrease of  $\alpha$ -helix from 61% (free BSA) to 36% (retinol) and 26% (retinoic acid) with an increase in random and turn structure (Fig. 2B and C and Table 1). These results are consistent with the decrease in the intensity of the protein amide I band discussed above. The major decrease in  $\alpha$ -helix structure and increase in random coil and turn structures suggest a partial protein unfolding at high retinoid concentrations.

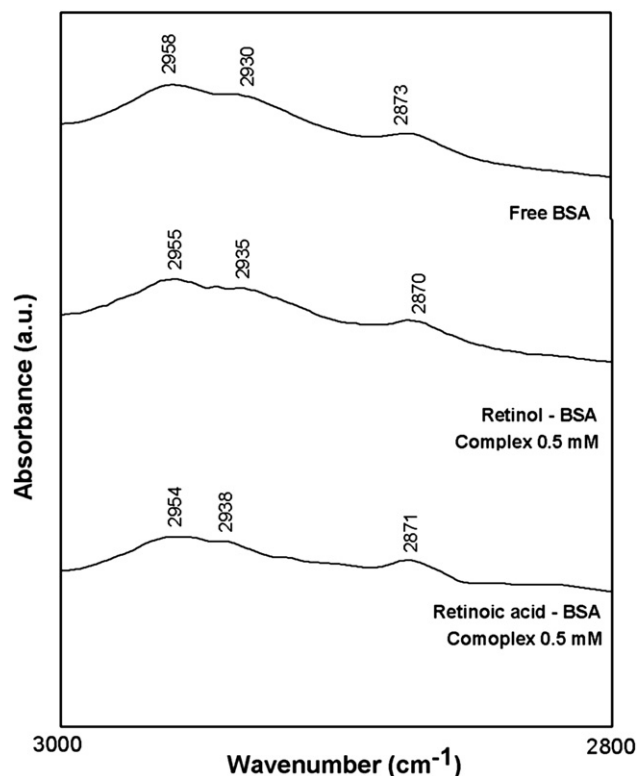


**Fig. 3.** Spectral changes for protein CH<sub>2</sub> symmetric stretching vibrations upon retinoid complexation.

### 3.2. CD spectra

The conformational changes observed from infrared results for BSA and its retinoid complexes are consistent with CD spectroscopic analysis shown in Table 2. The CD results show that free BSA has a high  $\alpha$ -helix content 62%,  $\beta$ -sheet 13%, turn 12% and random coil 13% (Table 2), consistent with the literature report [33]. Upon retinoid complexation, major reduction of  $\alpha$ -helix was observed from 62% in free BSA to 52% in retinol- and 44% in retinoic acid–BSA complexes (Table 2). The decrease in  $\alpha$ -helix was accompanied by an increase in the  $\beta$ -sheet, turn and random coil structures (Table 2). The major reduction of the  $\alpha$ -helix with an increase in the  $\beta$ -sheet, turn and random structures are consistent with the infrared results that showed reduction of  $\alpha$ -helix and increase of  $\beta$ -sheet and turn structures due to a partial protein unfolding (Tables 1 and 2).

### 3.3. Hydrophobic interactions

In order to examine the hydrophobic contact in the retinoid–protein complexes, the BSA antisymmetric and symmetric  $\text{CH}_2$  stretching vibrations [30] in the region  $3000\text{--}2800\text{ cm}^{-1}$  were used. The  $\text{CH}_2$  bands of the free BSA located at  $2958$ ,  $2930$  and  $2873\text{ cm}^{-1}$  shifted to  $2955$ ,  $2935$  and  $2870\text{ cm}^{-1}$  (retinol) and to  $2954$ ,  $2938$  and  $2871\text{ cm}^{-1}$  (retinoic acid) in the retinoid–protein

complexes (Fig. 3). The shifting of the protein antisymmetric and symmetric  $\text{CH}_2$  stretching vibrations suggests the presence of hydrophobic interactions *via* retinoid long chains and hydrophobic pockets in BSA [34]. Additional evidence for hydrophobic interaction comes from fluorescence spectroscopic results discussed below.

### 3.4. Fluorescence spectra and stability of retinoid–BSA complexes

BSA has two tryptophan residues that possess intrinsic fluorescence [10]. Trp-212 is located within a hydrophobic binding pocket of the protein and Trp-134 is located on the surface in the hydrophilic region of the molecule (Scheme 1). Tryptophan emission dominates BSA fluorescence spectra in the UV region. When other molecules interact with BSA, tryptophan fluorescence may change depending on the impact of such interaction on the protein conformation [11].

The decrease of fluorescence intensity of BSA is monitored at  $340\text{ nm}$  in retinoid–BSA systems (Fig. 4A and B show representative results for each system). The plot of  $F_0/F_0 - F$  vs  $1/[\text{retinoid}]$  is shown for retinoid–BSA complexes (Fig. 4A and 4B show representative plots). Assuming that the observed changes in fluorescence come from the interaction between retinoid and BSA, the quenching constant can be taken as the binding constant of the complex formation. The  $K$  values given here are averages of four-replicate and six-replicate runs for retinoid/BSA systems, each run involving several different concentrations of retinoid (Fig. 4A and B). The binding constants obtained were  $K_{\text{retinol-BSA}} = 5.3 (\pm 0.8) \times 10^6\text{ M}^{-1}$  and  $K_{\text{retinoic acid-BSA}} = 2.3 (\pm 0.4) \times 10^6\text{ M}^{-1}$  (Fig. 4A and B). The binding constants calculated for retinoid–BSA suggest strong affinity retinoid–BSA binding, compared to the other ligand–protein

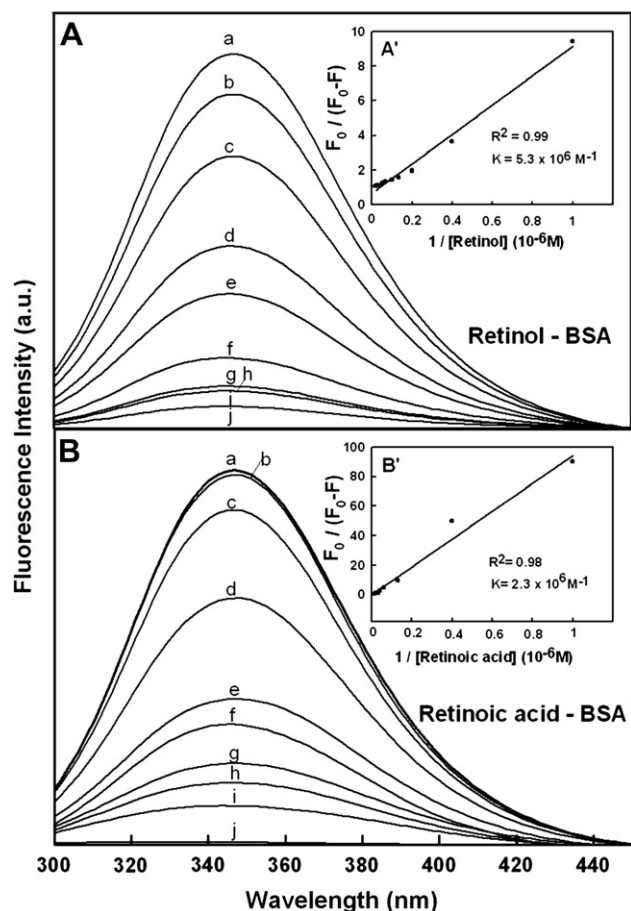


**Fig. 4.** Fluorescence emission spectra of retinoid–BSA systems in  $10\text{ mM}$  Tris–HCl buffer pH 7.4 at  $25\text{ }^{\circ}\text{C}$  presented for (A) retinol–BSA: (a) free BSA ( $7.5\text{ }\mu\text{M}$ ), (b–i) with retinol at  $1, 2.5, 10, 15, 20, 30, 40$  and  $60\text{ }\mu\text{M}$  (j) free retinol; (B) retinoic acid–BSA: (a) free BSA ( $7.5\text{ }\mu\text{M}$ ), (b–i) retinoic acid at  $1, 2.5, 10, 15, 20, 30, 40$  and  $60\text{ }\mu\text{M}$ , (j) free retinoic acid. Insert: The plot of  $F_0/F_0 - F$  as a function of  $1/\text{retinoid}$  concentration for A' (retinol) and B' (retinoic acid).

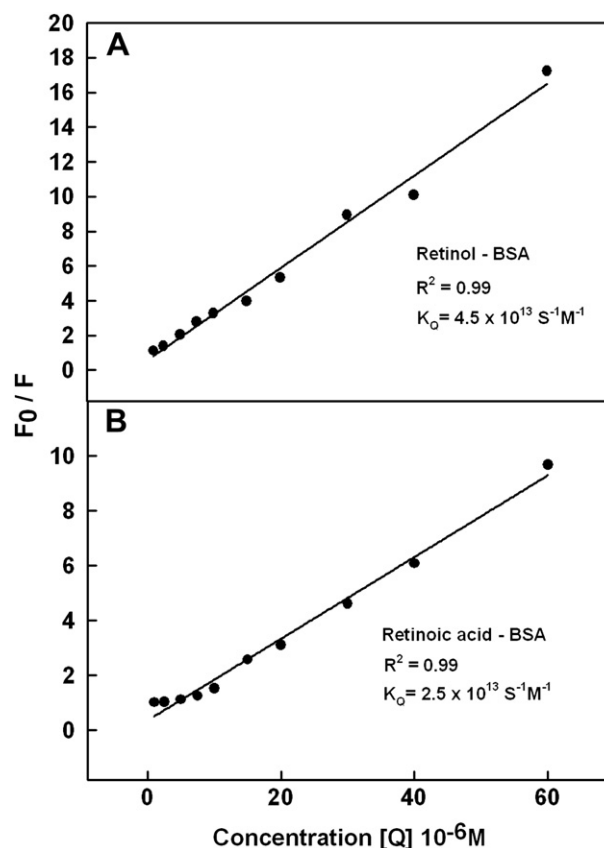


**Fig. 5.** Stern–Volmer plots for fluorescence quenching of the retinoid–BSA complexes at different retinoid concentrations (A) retinol–BSA and (B) retinoic acid–BSA.

complexes [34,35]. However, lower binding constants ( $10^4 \text{ M}^{-1}$  to  $10^3 \text{ M}^{-1}$ ) were also reported for several other ligand–protein complexes using fluorescence spectroscopic methods [20–25].

The lack of shifting of the tryptophan emission band at 340 nm upon retinol and retinoic acid interaction, is indicative of tryptophan molecules not exposed to any change in polarity (Fig. 4A and B). However, the bindings of retinoids are located in the vicinity of Trp-212 (buried inside) with hydrophobic contact and Trp-134 (on the surface) with hydrophilic contact. This argument is consistent with the molecular modeling, which shows the participation of both Trp-212 and Trp-134 in retinoid–BSA bindings (docking will be discussed further on). Similarly, infrared analysis of protein  $\text{CH}_2$  antisymmetric and symmetric stretching vibrations showed hydrophobic contact in retinoid–BSA complexes (Fig. 3). Evidence for hydrophilic interaction was discussed in the infrared section (Fig. 1).

In order to verify the presence of static or dynamic quenching in retinoid–BSA complexes we have plotted  $F_0/F$  against  $Q$  and the results are shown in Fig. 5. The plot of  $F_0/F$  vs  $Q$  is a straight line for retinoid–BSA adducts indicating that the quenching is mainly static in these retinoid–protein complexes [25]. The  $K_Q$  was estimated according to the Stern–Volmer equation:

$$F_0/F = 1 + K_Q t_0 [Q] = 1 + K_D [Q] \quad (8)$$

where  $F_0$  and  $F$  are the fluorescence intensities in the absence and presence of quencher,  $[Q]$  is the quencher concentration and  $K_D$  is the Stern–Volmer quenching constant, which can be written as  $K_D = k_Q t_0$ ; where  $k_Q$  is the bimolecular quenching rate constant and

$t_0$  is the lifetime of the fluorophore in the absence of quencher 5.9 ns [10,25,36]. The quenching constants ( $K_Q$ ) are  $4.5 \times 10^{13} \text{ M}^{-1}/\text{s}$  for retinol–BSA,  $2.5 \times 10^{13} \text{ M}^{-1}/\text{s}$  for retinoic acid–BSA adducts (Fig. 5).

The number of retinol and retinoic acid molecules bound per protein ( $n$ ) is calculated from  $\log [(F_0 - F)/F] = \log K + n \log [\text{retinoid}]$  for the static quenching [37–41]. The linear plot of  $\log [(F_0 - F)/F]$  as a function of  $\log [\text{retinoid}]$  is shown in Fig. 6. The  $n$  values from the slope of the straight line are 1.2 for retinol and 1.8 for retinoic acid (Fig. 6A and B). It seems that more than one molecule of the retinoid bind BSA, in these retinoid–protein complexes (Fig. 6).

It should be noted that our IR and CD spectroscopic measurements were carried out in a 25% ethanolic solution, while fluorescence spectra were recorded in 10% ethanol. In order to show that 25% ethanol has no effect on protein structure, we recorded the IR spectra of the free BSA in  $\text{H}_2\text{O}$  and in 25% ethanolic solution and the results are shown in Fig. 7. The spectra of BSA in water and in 25% ethanol are very similar with amide I band at 1659 ( $\text{H}_2\text{O}$ ),

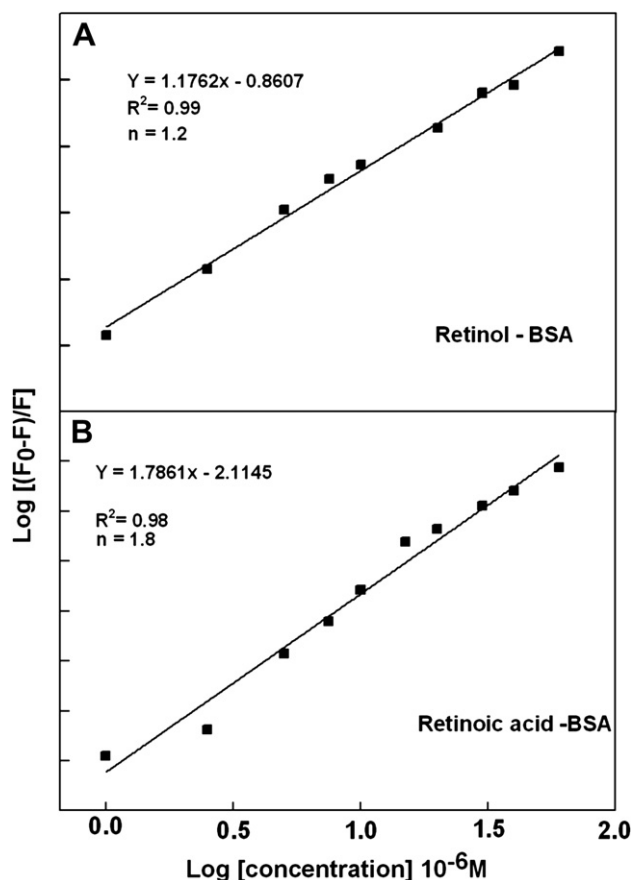


Fig. 6. The plot of  $\log (F_0 - F)/F$  as a function of  $\log (\text{retinoid concentration})$  for determination of the number of bound retinoid molecules per BSA ( $n$ ).

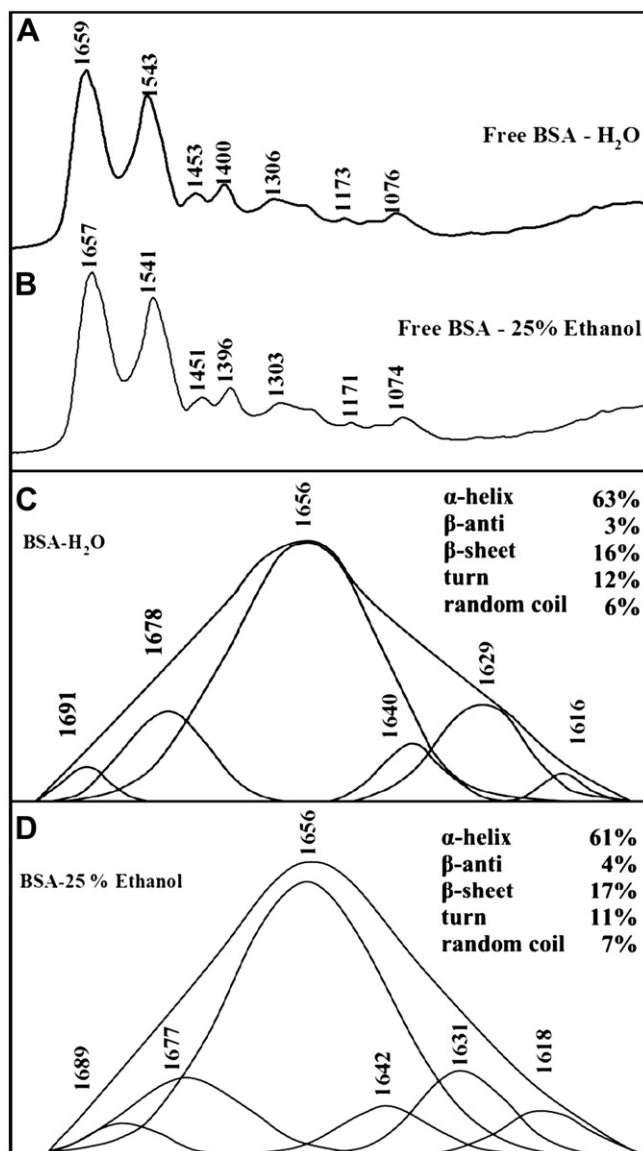
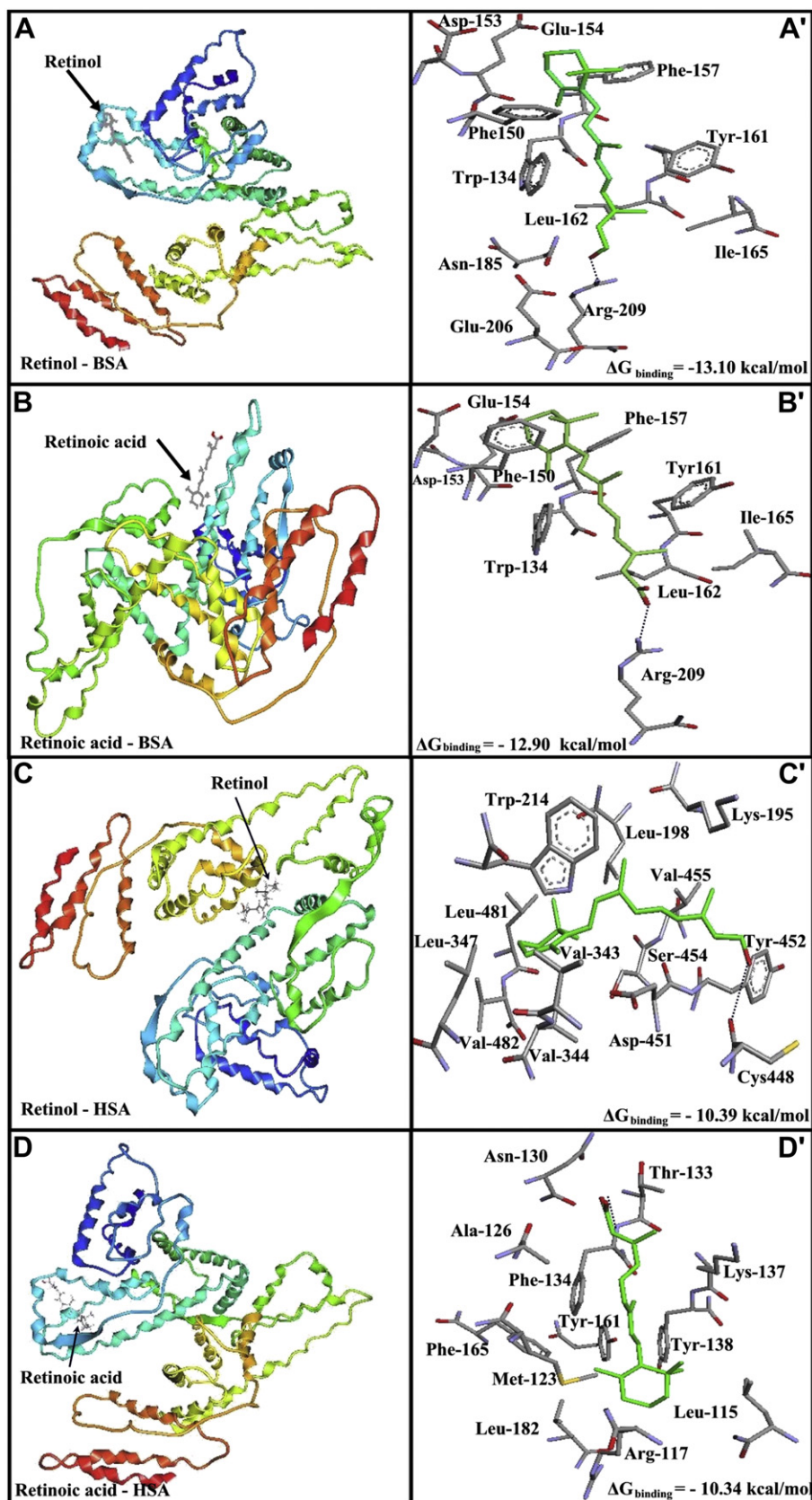


Fig. 7. Infrared spectra of the free BSA in water (A) and in 25% ethanol (B) and curve-fitted amide I band for protein conformation in water (C) and 25% ethanol (D) in the region of  $1800\text{--}600 \text{ cm}^{-1}$ .



**Fig. 8.** Best docked conformations of retinoid–BSA and retinoid–HSA complexes. (A) for retinol complexed to BSA, (B) for retinoic acid complexed to BSA, (C) for retinol complexed to HSA, (D) for retinoic acid complexed to HSA.



**Table 3**

Amino acid residues involved in retinoid–BSA and retinoid–HSA complexes with the free binding energy for the best selected docking positions.

Complex		$\Delta G_{\text{binding}}$ (kcal/mol)
Retinol–BSA	*Arg-209, Asn-185, Asp-153, Glu-154, Glu-206, Ile-165, Leu-162, Phe-150, Phe-157, Trp-134, Tyr-161	–13.10
Retinoic acid–BSA	*Arg-209, Asp-153, Glu-154, Ile-165, Leu-162, Phe-150, Phe-157, Trp-134, Tyr-161	–12.90
Retinol–HSA	Asp-451, *Cys-448, Leu-198, Leu-347, Leu-481, Lys-195, Ser-454, Trp-214, Tyr-452, Val-343, Val-344, Val-455, Val-482	–10.39
Retinoic acid–HSA	Ala-126, Arg-117, Asn-130, Leu-115, Leu-182, Lys-137, Met-123, *Phe-134, Phe-165, Thr-133, Tyr-138, Tyr-161	–10.34

\*Hydrogen bonding was observed with this residue.

1657  $\text{cm}^{-1}$  (25% ethanol) and amide II band at 1543 ( $\text{H}_2\text{O}$ ) and 1541  $\text{cm}^{-1}$  (25% ethanol) (Fig. 7A and B). The curve-fitted amide I band show almost similar percentages for protein conformation in water and in 25% ethanol with  $\alpha$ -helix 63% ( $\text{H}_2\text{O}$ ), 61% (25% ethanol),  $\beta$ -sheet 16% ( $\text{H}_2\text{O}$ ), 17% (25% ethanol), turn 12% ( $\text{H}_2\text{O}$ ), 11% (25% ethanol), random coil 6% ( $\text{H}_2\text{O}$ ), 7% (25% ethanol) and  $\beta$ -anti 3% ( $\text{H}_2\text{O}$ ) and 4% (25% ethanol) (Fig. 7C and D). As one can see marked similarities are observed for protein conformation in water and in 25% ethanol (with  $\pm 1$ –2% margin of error) indicating that 25% ethanol does not alter BSA conformation in our investigation (as mentioned in the Experimental section).

### 3.5. Docking studies and comparison between retinoid–BSA and retinoid–HSA complexes

Our FTIR, UV–visible, CD and fluorescence spectroscopic results were complemented with docking experiments in which retinoids were docked to BSA and HSA to determine the preferred binding sites for retinol and retinoic acid. The spectroscopic analysis of retinol and retinoic acid complexes with HSA has been previously reported [5]. However no attempt was made to locate the binding sites of retinoids with HSA using molecular modeling. The docking results shown in Fig. 8 and Table 3 are related to both retinoid–BSA and retinoid–HSA complexes. In the retinoid–BSA complexes, retinol is surrounded by \*Arg-209 (2.50 Å = H-bond), Leu-162 (2.38 and 2.42 Å), Phe-150 (1.89 Å), Phe-157 (2.14 and 2.42 Å), Trp-134 (2.52 and 2.39 Å) and Tyr-161 (1.81 Å) with the binding energy of 13.10 kcal/mol (Fig. 8 and Table 3). Similarly, retinoic acid is surrounded by \*Arg-209 (2.53 Å = H-bond), Ile-165 (2.10 Å), Leu-162 (2.46 and 2.31 Å), Phe-150 (2.16 Å), Phe-157 (1.99 Å), Trp-134 (2.55 Å) and Tyr-161 (2.14 Å) with the free binding energy of 12.90 kcal/mol (Fig. 8 and Table 3). On the other hand, in the retinoid–HSA complexes, retinol is surrounded by Asp-451 (1.83 Å), \*Cys-448 (2.79 Å = H-bond), Leu-347 (2.12 Å), Lys-195 (2.00 Å), Trp-214 (2.03 Å), Val-344 (2.14 Å), Val-455 (2.05 and 2.48 Å) and Val-482 (2.14 Å) with the free binding energy of 10.39 kcal/mol (Fig. 8 and Table 3). Similarly, retinoic acid is surrounded by Asn-130 (2.09 Å), \*Phe-134 (2.49, 2.53 and 2.67 Å = H-bond), Thr-133 (2.31 and 2.17 Å), and Tyr-161 (1.78, 1.92 and 2.22 Å) with the free binding energy of 10.34 kcal/mol (Fig. 8 and Table 3). It is evident that several amino acids with hydrophobic and hydrophilic characters are in contact with retinoid in these HSA and BSA complexes (Fig. 8 and Table 3). Molecular modeling presented in Table 3 shows major differences in the binding sites of retinol and retinoic acid complexes with HSA and BSA (different amino acids are involved in retinoid–protein complexation). Spectroscopic data showed major alterations of BSA conformation, upon retinol and retinoic acid complexation leading to protein unfolding, whereas HSA secondary structure was stabilized by retinoid interaction [5] indicating of a different mode of bindings of retinoids to BSA and HSA. In fact docking studies showed different amino acids were involved in retinoid binding to BSA and HSA with more stable complexes formed with BSA (Table 3). However, spectroscopic results showed BSA and HSA form more stable complexes with retinol than retinoic acid  $K_{\text{retinol-BSA}} = 5.3 \times 10^6 \text{ M}^{-1}$ ,

$K_{\text{retinoic acid-BSA}} = 2.3 \times 10^6 \text{ M}^{-1}$ ,  $K_{\text{retinol-HSA}} = 1.3 \times 10^5 \text{ M}^{-1}$  and  $K_{\text{retinoic acid-HSA}} = 3.3 \times 10^5 \text{ M}^{-1}$  [5]. It should be noted that the results from docking are qualitative at best and they should only be compared with themselves (like docking multiple ligands on the same binding site should tell us which one is the best when comparing the results together) and not to compare with spectroscopic results (quantitative data) obtained on retinoid–protein interactions.

## 4. Conclusion

In summary, retinoids strongly bind serum albumins with more stable complexes formed with BSA than HSA (based on modeling). Retinoid interaction with BSA alters protein secondary structure leading to protein unfolding, while HSA conformation was stabilized by retinoid complexation. The results can support the effective transportation of retinoids *via* serum albumins and the effect of bovine serum albumin on the uptake of retinoic acid *in vivo*, which reduces significantly the isomerization of all *cis*-retinoic acid to all *trans*-retinoic acid.

## Acknowledgments

This work is supported by a grant from Natural Sciences and Engineering Research Council of Canada (NSERC) to H.A. Tajmir-Riahi.

## References

- [1] M. Tsukada, M. Schroder, H. Seltmann, C.E. Orfanos, C.C. Zouboutis, J. Invest. Dermatol. 119 (2002) 182–185.
- [2] C. Folli, V. Calderone, S. Ottonello, A. Bolchi, G. Zanotti, M. Stoppini, R. Berni, Proc. Natl. Acad. Sci. U.S.A. 98 (2001) 3710–3715.
- [3] S. Vogel, C.L. Mandelsohn, J.R. Mertz, R. Piantadosi, C. Waldburger, M.E. Gottesman, W.S. Blaner, J. Biol. Chem. 276 (2001) 1353–1360.
- [4] D.E. Ong, B. Kakkad, P.N. MacDonald, J. Biol. Chem. 262 (1987) 2729–2736.
- [5] C.N. N'soukpoe-Kossi, R. Sedaghat-Herati, C. Ragi, S. Hotchandani, H.A. Tajmir-Riahi, Int. J. Biol. Macromol. 40 (2007) 484–490.
- [6] D.C. Carter, J.X. Ho, Adv. Protein Chem. 45 (1994) 153–203.
- [7] T. Peters, All About Albumin. Biochemistry, Genetics and Medical Applications, Academic Press, San Diego, 1996.
- [8] X.M. He, D.C. Carter, Nature 358 (1992) 209–215.
- [9] T. Peters, Serum albumin, Adv. Protein Chem. 37 (1985) 161–245.
- [10] N. Tayeh, T. Rungassamy, J.R. Albani, J. Pharm. Biomed. Anal. 50 (2009) 107–116.
- [11] J.R. Lakowicz, Principles of Fluorescence Spectroscopy, third ed, Springer, New York, 2006.
- [12] L. Painter, M.M. Harding, P.J. Beeby, J. Chem. Soc. Perkin Trans. 18 (1998) 3041–3044.
- [13] S.Y. Lin, M.J. Li, Y.S. Wei, Spectrochim. Acta Part A 60 (2004) 3107–3111.
- [14] F. Dousseau, M. Therrien, M. Pezolet, Appl. Spectrosc. 43 (1989) 538–542.
- [15] D.M. Byler, H. Susi, Biopolymers 25 (1986) 469–487.
- [16] R. Beauchemin, C.N. N'soukpoe-Kossi, T.J. Thomas, T. Thomas, R. Carpentier, H.A. Tajmir-Riahi, Biomacromolecules 8 (2007) 3177–3183.
- [17] A. Ahmed, H.A. Tajmir-Riahi, R. Carpentier, FEBS Lett. 363 (1995) 65–68.
- [18] W.C. Johnson, Proteins Struct. Funct. Genet. 35 (1999) 307–312.
- [19] N. Sreerama, R.W. Woody, Anal. Biochem. 287 (2000) 252–260.
- [20] C. Dufour, O. Dangles, Biochim. Biophys. Acta 1721 (2005) 164–173.
- [21] E. Froehlich, C.J. Jennings, M.R. Sedaghat-Herati, H.A. Tajmir-Riahi, J. Phys. Chem. B 113 (2009) 6986–6993.
- [22] W. He, Y. Li, C. Xue, Z. Hu, X. Chen, F. Sheng, Bioorg. Med. Chem. 13 (2005) 1837–1845.
- [23] C.Q. Jiang, M.X. Gao, J.X. He, Anal. Chim. Acta 452 (2002) 185–189.

- [24] S. Bi, L. Ding, Y. Tian, D. Song, X. Zhou, X. Liu, H. Zhang, J. Mol. Struct. 703 (2004) 37–45.
- [25] J. Min, M.X. Xia, D. Zheng, Y. Liu, X.Y. Li, X. Chen, J. Mol. Struct. 692 (2004) 71–80.
- [26] K. Arnold, A.K. Bordoli, L. Kopp, T. Schwede, *Bioinformatics* 22 (2006) 195–201.
- [27] B. Rost, *Protein Eng.* 12 (1999) 85–94.
- [28] S. Sugio, A. Kashima, S. Mochizuki, M. Noda, K. Kobayashi, *Protein Eng.* 12 (1999) 439–446.
- [29] T. Schwede, J. Kopp, N. Guex, M.C. Peitsch, *Nucleic Acids Res.* 31 (2003) 3381–3385.
- [30] S. Krimm, J. Bandekar, *Adv. Protein Chem.* 38 (1986) 181–364.
- [31] A. Ahmed Ouameur, S. Diamantoglou, M.R. Sedaghat-Herati, Sh. Nafisi, R. Carpentier, H.A. Tajmir-Riahi, *Cell. Biochem. Biophys.* 45 (2006) 203–213.
- [32] J. Tian, J. Liu, Z. Hu, X. Chen, *Am. J. Immunol.* 1 (2005) 21–23.
- [33] J. Grdadolnik, *Acta Chim. Slov.* 50 (2003) 777–788.
- [34] S. Dubeau, P. Bourassa, T.J. Thomas, H.A. Tajmir-Riahi, *Biomacromolecules* 11 (2010) 1507–1515.
- [35] U. Kragh-Hansen, *Dan. Med. Bull.* 37 (1990) 57–84.
- [36] N.A. Kratochwil, W. Huber, F. Muller, M. Kansy, P.R. Gerber, *Biochem. Pharmacol.* 64 (2002) 1355–1374.
- [37] Zu-De. Qi, B. Zhou, Q. Ziao, C. Shi, Y. Liu, J. Dei, J. *Photochem. Photobiol. A* 193 (2008) 81–88.
- [38] L. Liang, H.A. Tajmir-Riahi, M. Subirade, *Biomacromolecules* 9 (2008) 50–55.
- [39] D. Charbonneau, M. Beauregard, H.A. Tajmir-Riahi, *J. Phys. Chem. B* 113 (2009) 1777–1784.
- [40] J.S. Mandeville, E. Froehlich, H.A. Tajmir-Riahi, *J. Pharm. Biomed. Anal.* 49 (2009) 468–474.
- [41] J.S. Mandeville, H.A. Tajmir-Riahi, *Biomacromolecules* 11 (2010) 465–472.